



Iterative reconstruction algorithm improves the image quality without affecting quantitative measurements of computed tomography perfusion in the upper abdomen

Mischa Woisetschläger^{a,b,*}, Lilian Henriksson^{a,b}, Wolf Bartholomae^{a,b}, Thomas Gasslander^c, Bergthor Björnsson^c, Per Sandström^c

^a Department of Radiology in Linköping, and Department of Health, Medicine and Caring Sciences, Linköping University, Linköping, Sweden

^b Center for Medical Image Science and Visualization (CMIV), Linköping University, Linköping, Sweden

^c Department of Surgery in Linköping, and Department of Biomedical and Clinical Sciences, Linköping University, Linköping, Sweden

ARTICLE INFO

Keywords:

4D computed tomography
Perfusion
Abdomen
Image reconstruction
Radiation dosage
Liver

ABSTRACT

Objective: To investigate differences between reconstruction algorithms in quantitative perfusion values and time-attenuation curves in computed tomography perfusion (CTP) examinations of the upper abdomen.

Methods: Twenty-six CTP examinations were reconstructed with filtered back projection and an iterative reconstruction algorithm, advanced modeled iterative reconstruction (ADMIRE), with different levels of noise-reduction strength. Using the maximum-slope model, quantitative measurements were obtained: blood flow (mL/min/100 mL), blood volume (mL/100 mL), time to peak (s), arterial liver perfusion (mL/100 mL/min), portal venous liver perfusion (mL/100 mL/min), hepatic perfusion index (%), temporal maximum intensity projection (Hounsfield units (HU)) and temporal average HU. Time-attenuation curves for seven sites (left liver lobe, right liver lobe, hepatocellular carcinoma, spleen, gastric wall, pancreas, portal vein) were obtained. Mixed-model analysis was used for statistical evaluation. Image noise and the signal:noise ratio (SNR) were compared between four reconstructions, and statistical analysis of these reconstructions was made with a related-samples Friedman's two-way analysis of variance by ranks test.

Results: There were no significant differences for quantitative measurements between the four reconstructions for all tissues. There were no significant differences between the AUC values of the time-attenuation curves between the four reconstructions for all tissues, including three automatic measurements (portal vein, aorta, spleen). There was a significant difference in image noise and SNR between the four reconstructions.

Conclusions: ADMIRE did not affect the quantitative measurements or time-attenuation curves of tissues in the upper abdomen. The image noise was lower, and the SNR higher, for iterative reconstructions with higher noise-reduction strengths.

1. Introduction

Computed tomography perfusion (CTP) has been used since 1991, but broad application of this modality in clinical workflow has not been implemented. This is due (at least in part) to: (i) the initially limited area that could be examined; (ii) quality issues because of motion artifacts from breathing; (iii) the high radiation doses rendered by these

studies compared with standard CT.

More recently, technological developments in CT have made it possible to increase the scan length for CTP, thereby enabling coverage of the entire trunk. They have also provided effective ways to eliminate motion artefacts that are otherwise problematic in CTP examinations of this body area.

Another important aspect to ensuring wider acceptance of CTP by

Abbreviations: CTP, computed tomography perfusion; FBP, filtered back projection; ADMIRE, advanced modelled iterative reconstruction; TAC, time attenuation curve; TACE, transarterial chemoembolization; GFR, glomerular filtration rate; AUC, area under the curve; SNR, signal to noise ratio; ALP, arterial liver perfusion; BF, blood flow; BV, blood volume; TTP, time to peak; PVP, portal venous liver perfusion; HPI, hepatic perfusion index; BMI, body mass index; HCC, hepatocellular carcinoma; LI-RADS-5, liver imaging reporting and data system

* Corresponding author at: Department of Radiology in Linköping, and Department of Health, Medicine and Caring Sciences, Linköping University, 581 81, Linköping, Sweden.

E-mail address: mischa.woisetschlag@liu.se (M. Woisetschläger).

<https://doi.org/10.1016/j.ejro.2020.100243>

Received 11 May 2020; Received in revised form 17 June 2020; Accepted 19 June 2020

2352-0477/ © 2020 The Authors. Published by Elsevier Ltd. This is an open access article under the CC BY-NC-ND license (<http://creativecommons.org/licenses/by-nc-nd/4.0/>).

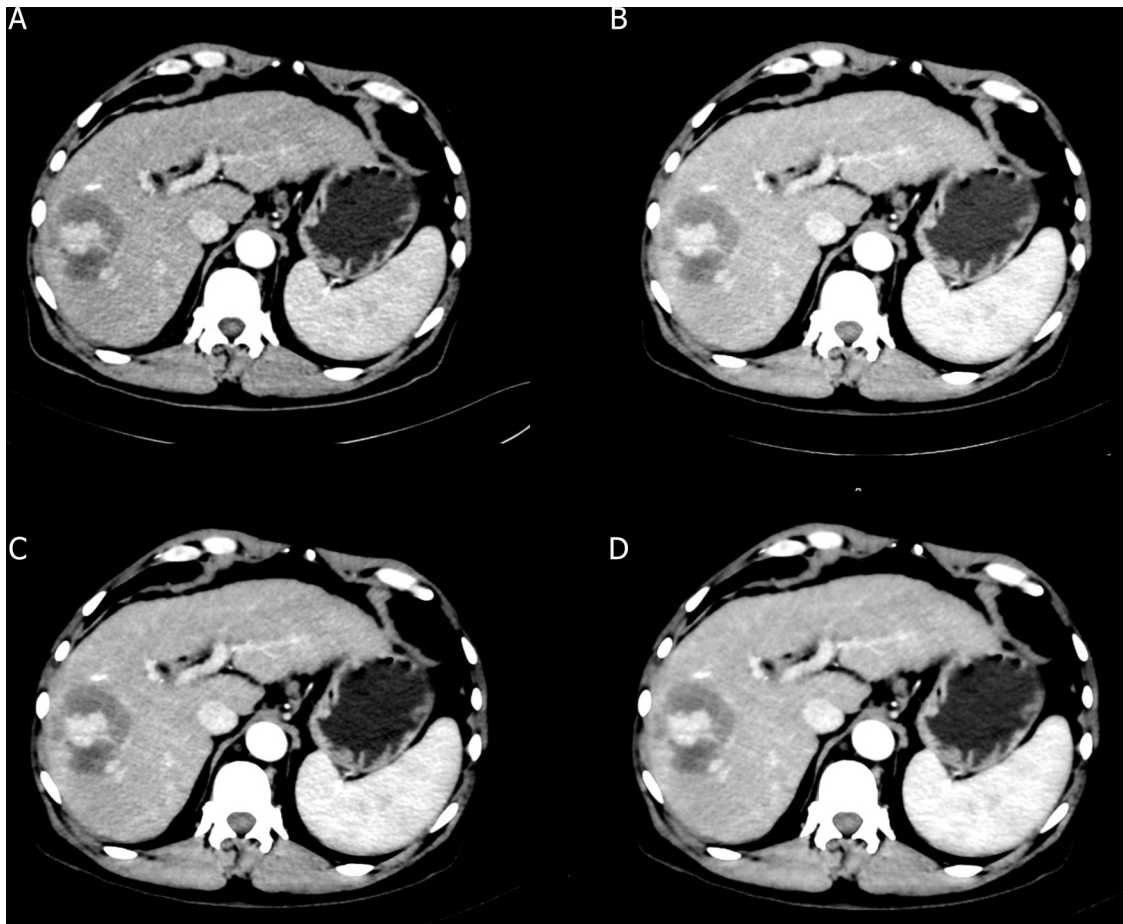


Fig. 1. Temporal Average Images (including all 25 time points after motion correction) reconstructed with FBP (A), ADM 3 (B), ADM4 (C) and ADM 5 (D).

radiologists is to increase the image quality to make visual assessment possible using the CTP dataset instead of having to rely on quantitative information alone. CTP examinations are reconstructed primarily with filtered back projection (FBP), so the image quality of the included multiple low-dose series is limited by default. Introduction of new iterative reconstruction algorithms that can improve the image quality by, for example, reduction of image noise, could be a solution in this context [1–3]. If applied along with lowering of the kVp, the radiation dose could be kept at a reasonable level while providing sufficient morphologic information. However, the quantitative information must not be altered by this strategy. Comparative studies of visual and quantitative assessments of CTP images are, therefore, warranted.

Recent studies have shown that iterative reconstruction algorithms can be used to reduce the radiation dose with preserved/increased image quality and retention of quantitative measurements in CTP examinations. However, most of those studies were undertaken in the brain [4,5], heart [6–9] or the lungs [10,11]. Only a few studies have been undertaken in the abdomen, such as the liver [12], pancreas [13] and colon [14]. Such studies of CTPs in the upper abdomen have not been carried out on a CT system built by Siemens Healthcare.

Iterative reconstruction kernels might increase the image quality of CTP examinations significantly. Hence, CTP might be used as a first-line modality to offer the advantages of quantitative information of different tissues.

We investigated if there are differences between quantitative measurements and the time-attenuation curves obtained in different tissues in reconstructions made with FBP and advanced modeled iterative reconstruction (ADMIRE) using a system from Siemens Healthcare.

2. Materials and methods

2.1. Ethical approval of the study protocol

This prospective study was approved by the regional ethics committee (dnr 2016-43-31). Informed consent was obtained from all patients.

2.2. Patient population

Nineteen patients (5 women; 14 men; mean age \pm standard deviation (SD), 70 ± 8.3 years; range, 55–86 years) with hepatocellular carcinoma (HCC) scheduled for transarterial chemoembolization (TACE) from October 2016 to March 2019 were included in the study. Seven patients had a follow-up examination that was also included, resulting in a total of 26 CTP studies. The follow-up CTP for these seven patients was carried out 3 weeks after TACE. Based on Liver Imaging Reporting and Data System (LI-RADS), all patients had LIRADS 5 lesions according to a previous CT study, and were scheduled to undergo TACE. Six patients died during the study period.

Inclusion criteria were patients with at least one LI-RADS-5 lesion and the ability to provide written informed consent. Exclusion criteria were patients regarded too sick to travel to our institution for follow-up CT, and with a reduced glomerular filtration rate (GFR).

2.3. CTP procedure

CTP examinations were undertaken on a Somatom Force scanner (Siemens Healthcare). The scanning parameters were a tube voltage of 70 kVp, tube current of 150 mA with collimation of 48×1.2 or

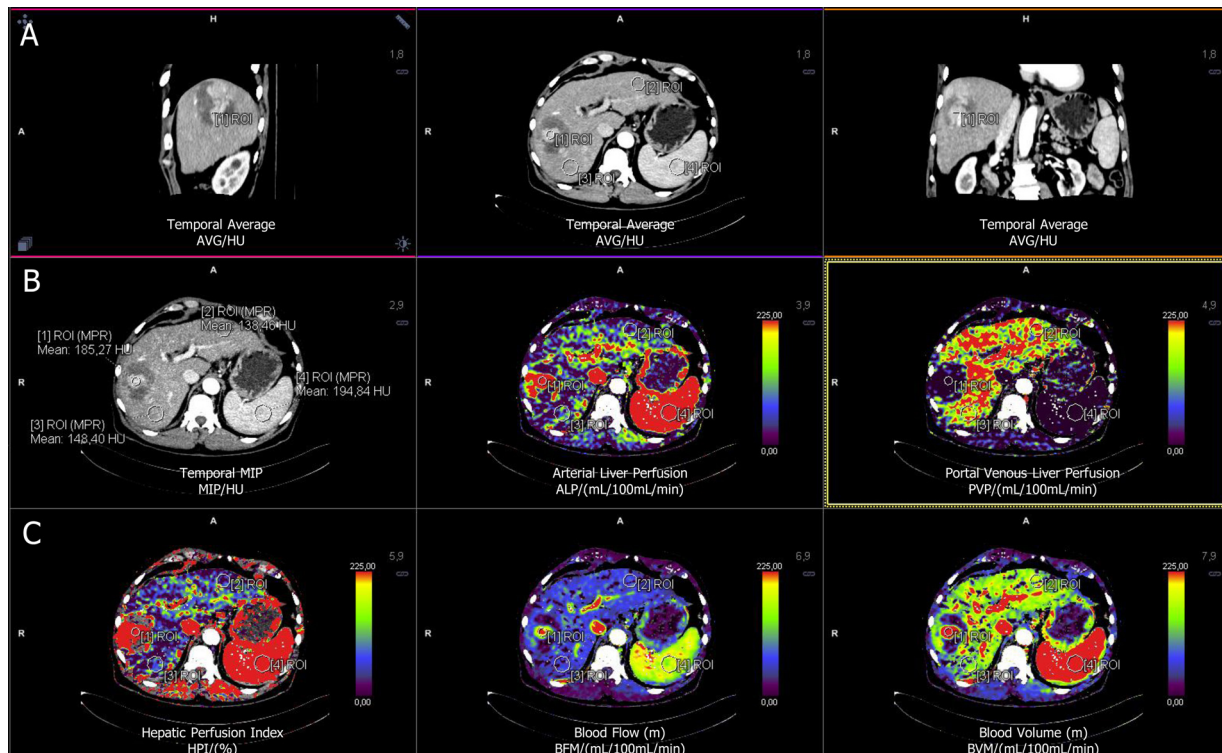


Fig. 2. Resulting images from syngo.Via. after reconstruction with FBP. Row A: Sagittal, axial and coronal Temporal Average reconstructions (all 25 time points after motion correction) with four ROIs (HCC (1), left liver lobe (2), right liver lobe (3), spleen (4)). Row B: MIP (Maximum Intensity Projektion), ALP (Arterial Liver Perfusion) and PVP (Portal Venous Perfusion) reconstructions with the four measurements at exactly the same position as in Row A, which is done automatically by syngo.Via. Row C: HPI (Hepatic Index), BFM (Blood Flow) and BVM (Blood Volume) reconstructions with the four measurements at exactly the same position as in Row A, which is done automatically by syngo.Via. (Only four of the seven tissues are shown for visibility reasons).

192 × 0.6 mm, for a total of 25 scans. The total scanning time was 45.45 s, with the first 20 scans made every 1.5 s and the last five scans undertaken every 3 s. The first scan was taken 8 s after injection of contrast material. The scan length was 22.4 cm. The scans were obtained with the patient moving back-and-forth through the gantry in a “pendulum” movement. Patients were instructed to take shallow breaths during imaging. A fixed dose of 50 mL of iopromide (Ultravist™; Bayer, Leverkusen, Germany) with a concentration of 370mgI/mL was injected at a flowrate of 6 mL/s followed by a flush of physiologic (0.9 %) saline (50 mL) at 6 mL/s with a dual-head power injector (Ulrich Medical, Ulm, Germany) with a maximum inflow time of 8 s. Compression to the upper abdomen was not applied. The mean dose length product per examination was 1168 mGycm, with an equivalent effective dose of 17.5 mSv (k factor: 0.015).

2.4. Image reconstruction

The raw data from the scan were reconstructed in four ways: FBP, ADMIRE noise-reduction level 3–5 (ADM 3, ADM 4 and ADM 5). The slice thickness for all series was 1.5 mm, with a convolution kernel of Bv40 (Fig. 1).

2.5. Image analyses

Image analyses were undertaken using the CT Body Perfusion module on a server-based workstation (syngo.Via version 5.1, Siemens Healthcare). The liver template was chosen, and automatic motion correction was applied. The maximum slope model was used for generation of quantitative measurements: blood flow (BF), blood volume (BV) and time to peak (TP). Results generated from the model consisted of arterial liver perfusion (ALP), portal venous liver perfusion (PVP) and hepatic perfusion index (HPI). In addition, measurements of

Hounsfield units (HU) in temporal maximum intensity projection (TMIP) and temporal average (TAVG) images were made.

After motion correction, a four-dimensional (4D) noise-reduction algorithm was applied in FBP and ADMIRE reconstructions, as suggested by the software. Vessel definition was done by placement of regions of interest (ROIs) in the aorta (for the arterial input function), spleen (detection of the start and endpoint of ALP) and portal vein (detection of maximum enhancement of the portal vein).

For all four reconstruction types, ROIs were placed in the following tissues: (i) left liver lobe, (ii) right liver lobe, (iii) spleen, (iv) gastric wall, (v) pancreas and (vi) portal vein (Fig. 2). This strategy generated quantitative information of BF (mL/min/100 mL), BV (mL/100 mL), TP (s), ALP (mL/100 mL/min), PVP (mL/100 mL/min), HPI (%), temporal MIP_HU (TMIP; HU) and temporal average_HU (TAVG; HU) (Fig. 3). ROIs were placed at approximately identical positions and had approximately identical size in all reconstructions.

The time curves of each ROIs were exported and analyzed statistically. In addition, the software provided time-attenuation curves automatically for the arterial input function (AIF_HU_syngo), spleen (Spleen_HU_syngo) and portal vein (Portal_Vein_HU_syngo). These parameters were exported and analyzed statistically.

2.6. Image quality

Quantitative parameters for image quality were obtained by measuring image noise and the signal:noise ratio (SNR) in time-averaged images. “Image noise” was defined as the average of the SDs measured in the respective organs. The SNR was calculated by dividing the mean of each ROI by the image noise in the same ROI (Eq. (1)):

$$SNR \text{ of Organ } X = \frac{\text{Mean HU of ROI of Organ } X}{\text{Standarddeviation of the ROI of Organ } X} \quad (1)$$



Fig. 3. TAC (A) and table (B) for four tissues with Filtered Back Projection (HCC (1), left liver lobe (2), right liver lobe (3), spleen (4)). On the X axis: time; Y axis: HU. In the table (B), the values for PVP (Portal Venous Perfusion); HPI (Hepatic Index); BFM (Blood Flow); BVM (Blood Volume) and TTPM (Time To Peak) for the four tissues are shown. TAC = Time Attenuation Curve. (Only four of the seven tissues are shown for visibility reasons).

2.7. Statistical analyses

Statistical analyses were carried out using SPSS v25 (IBM). Data were analyzed for a normal distribution using the Shapiro–Wilk test. Differences between the quantitative measurements in seven tissues from the four reconstruction types were analyzed by a mixed model. For analyses of differences between the time curves, the area under curve (AUC) was calculated, and then this value was used for the mixed-model analysis.

Measurements of image noise and the SNR were analyzed with a related-samples Friedman’s two-way analysis of variance by ranks test. Significant values were adjusted by the Bonferroni correction for multiple tests. P < 0.05 was considered significant.

3. Results

There was no significant difference between the quantitative measurements of BF, BV, TP, ALP, PVP, HPI or TAVG between the four reconstructions in any tissue (Fig. 4).

There was no significant difference between the AUC values of the time-attenuation curves between the four reconstructions in any tissue, including the three automatic measurements from the workflow (Fig. 5).

3.1. Image noise

With regard to image noise, there were significant differences between FBP and ADM 4, as well as FBP and ADM 5, for all organs (Table 1).

3.2. SNR

There were significant differences in the SNR between FBP and ADM 4, as well as FBP and ADM 5, for all organs (Table 2).

3.3. Demographics

The mean weight of patients was 89.7 ± 22.3 (range: 60–130) kg. The mean height was 176 ± 9.54 (range: 162–195) cm. The mean body mass index was 28.8 ± 6.42 (range 20–42) kg/m². The mean abdominal diameter at L2 was 37.1 ± 4.39 (range: 30.9–47.3) cm.

3.4. Dose

The mean radiation dose for CTP examinations was 17.5 ± 3.26 (range: 12.96–24.81) mSv.

4. Discussion

We showed that quantitative measurements and AUC measurements for different organs from four reconstruction kernels did not differ in a low-dose CTP protocol. The mean image noise was lower for iterative reconstruction kernels with stronger filters compared with FBP. The SNR increased with stronger iterative reconstruction kernels compared with FBP.

If the image quality from a CTP examination of the abdomen was sufficient for disease detection, it could enable CTP to become a first-line examination. Then, CTP could provide quantitative information about lesions that might help their characterization and, possibly, the prediction of outcome. Blood vessels could be visualized optimally by

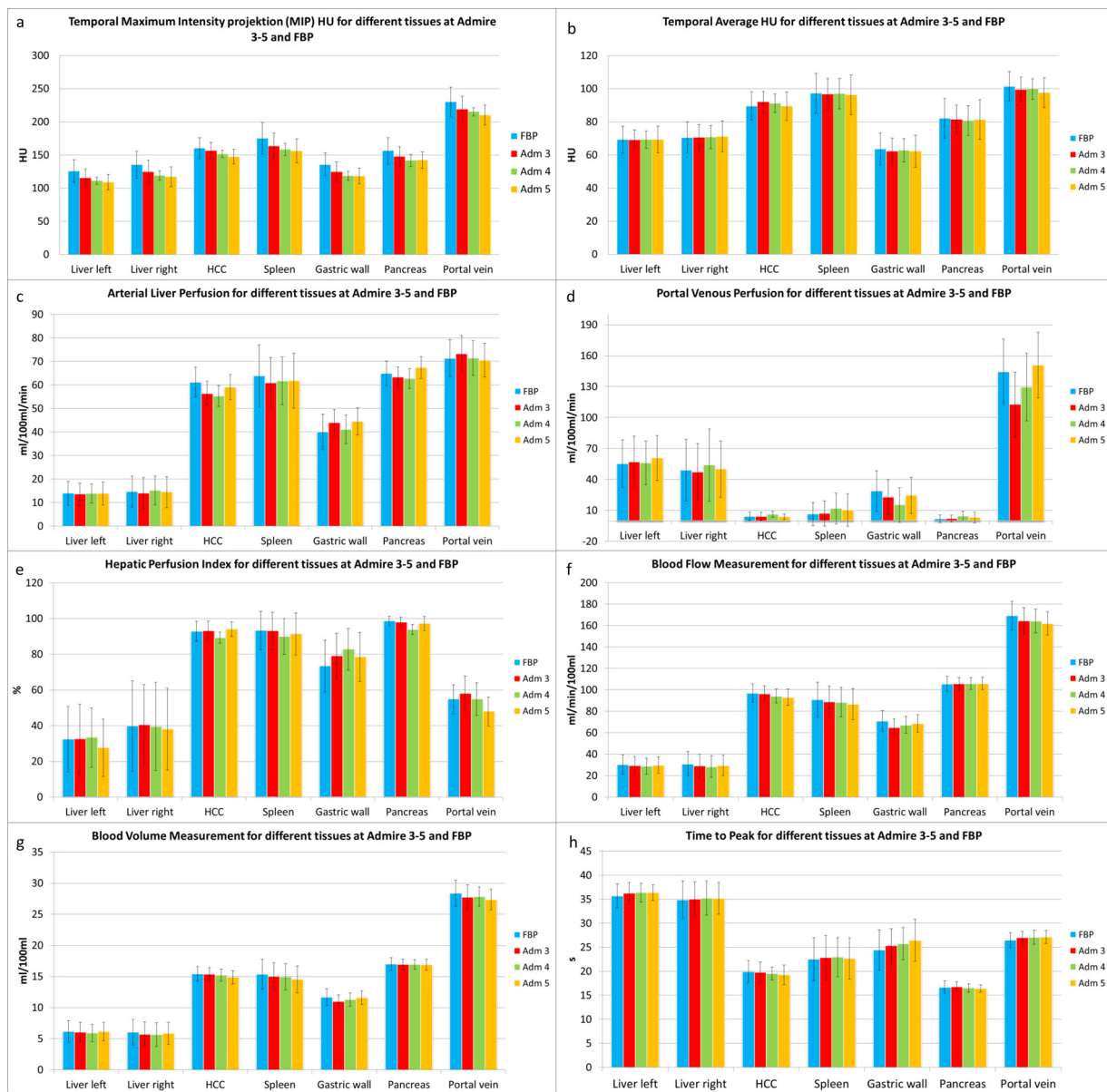


Fig. 4. Quantitative measurements (a: HU of the temporal MIP projection; b: HU of the temporal average projection; c: arterial liver perfusion (ml/100 mL/min); d: portal venous perfusion (ml/100 mL/min); e: hepatic perfusion index (%); f: blood flow (mL/100 mL/min); g: blood volume (mL/ 100 mL) and h: time to peak (s)) of seven sites (left liver lobe, right liver lobe, HCC, spleen, gastric wall, pancreas and portal vein) with four reconstruction kernels (FBP, ADM 3, ADM 4, ADM5) including values for standard deviation. No significant differences were found for all measurements and tissues between the four algorithms.

TMIP methods before TACE, surgery or other interventional procedures. Contrast phases could be optimized with regard to timing, which would overcome the shortcomings of fixed-timing and bolus-tracked protocols. In protocols with fixed timing or bolus tracking, cardiac output, inspiration grade, hepatic cirrhosis, vessel calcifications, hypovolemia, renal function, weight, height, age, and sex can affect the optimal timing for imaging [15]. Early and late arterial phases are susceptible to these factors, and CTP might overcome these difficulties by providing the optimal timing retrospectively using the arterial input function. As the vascular enhancement is directly proportional to the iodine delivery rate (2,2 gI/s) it is important to keep a high flow rate, as explained by Renko et al. [16,17] This will provide optimal contrast in the early and late arterial phase of the examination. In order for CT perfusion examination calculations to function the injection time should be short, as longer injection times can disturb the correct crossing time point of the arterial and portal venous time attenuation curves [18]. A CTP examination with comparable image quality and

radiation dose to a 3–4-phase examination of the upper abdomen could also be used if there is a strong suspicion of lesions in the upper abdomen but where the origin is not clear. One of the major reasons why CTP of the abdomen is not used more widely is the high radiation dose it entails [18,19]. One way of lowering the radiation dose is to use iterative reconstruction algorithms and a lower kVp. We employed a radiation dose of 17.5 mSv, which is comparable with a four-phase CT scan with 120 kV in our clinic. We believe that this radiation dose might be acceptable for lesion detection using CTP. Further investigation is needed to ascertain if a CTP examination can show the same prevalence of lesion detection as that of a comparable four-phase CT examination. This issue will be investigated by our research team in the future.

Perfusion parameters have been shown to be helpful for tumor characterization [20]. Hence, it might be beneficial to use CTP as a first-line examination as long as the image quality is sufficient for visual assessment (i.e., lesion detection and qualitative parameters are not altered). Perfusion parameters may serve as valuable tools for the non-

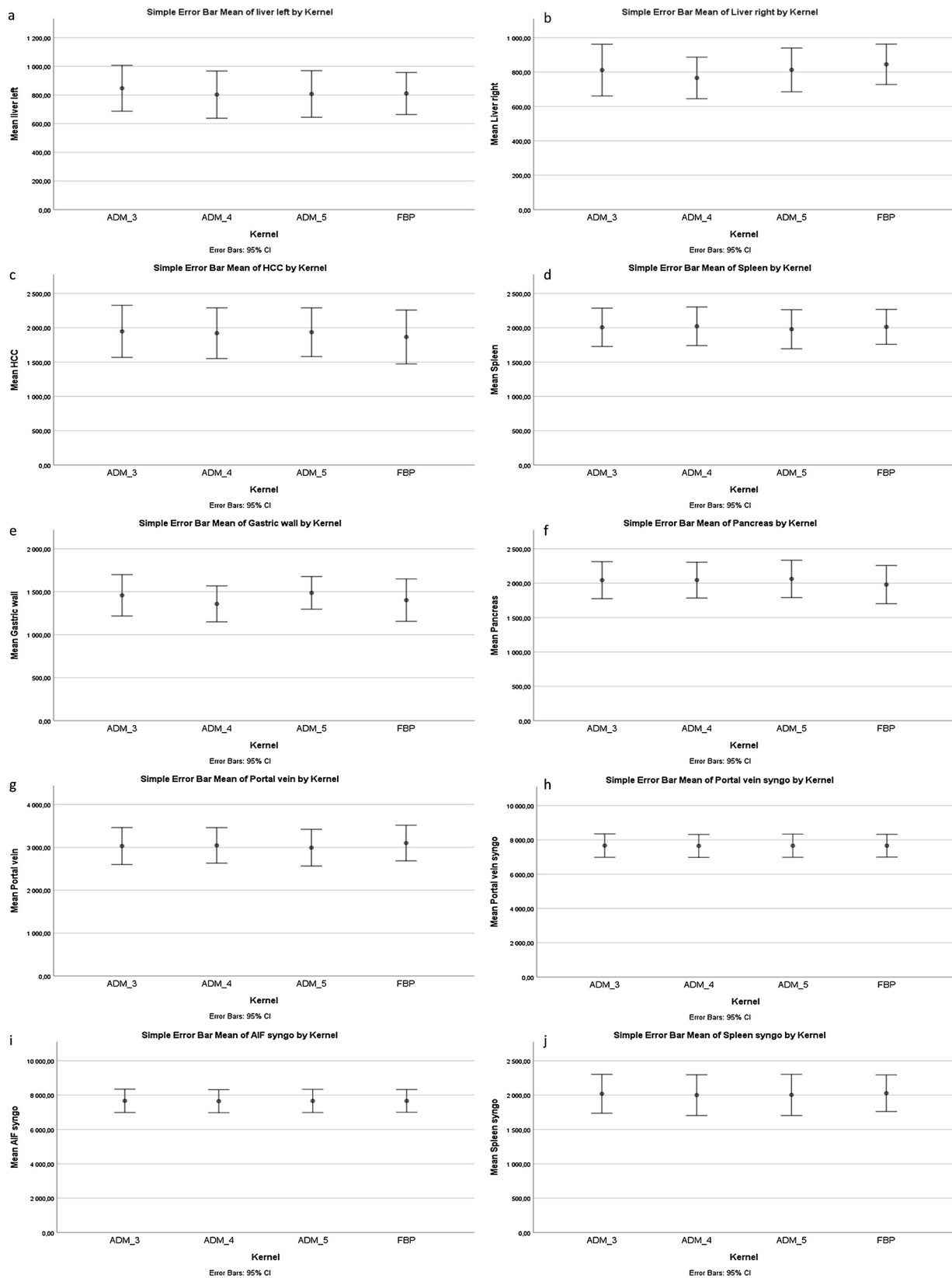


Fig. 5. Mean values of the area under the curve for 10 tissues (a: left liver lobe; b: right liver lobe; c: HCC; d: spleen; e: gastric wall; f: pancreas; g: portal vein (manual measurement); h: portal vein syngo (automatic measurement by syngo.Via); i: arterial input function syngo (AIF syngo; automatic measurement by syngo.Via in the aorta); j: spleen syngo (automatic measurement by syngo.Via) for four kernels (FBP, ADM 3, ADM 4, ADM 5) with values for standard deviations. No significant differences were found for all measurements and tissues between the four algorithms.

Table 1

Mean noise values (including ranges) for seven tissues (left liver lobe, right liver lobe, HCC, spleen, gastric wall, pancreas and portal vein) for four reconstruction algorithms (FBP, ADM 3, ADM 4, ADM 5).

| | Mean (95 % confidence interval) | | | | P-value |
|--------------|---------------------------------------|----------------------------------|---------------------|---------------------|---------|
| | FBP | ADM 3 | ADM 4 | ADM 5 | |
| Noise (HU) | | | | | |
| Liver left | 8,09 (5,76 - 11,6) ^{a,b,c} | 6,15 (3,64 - 9,28) ^e | 5,30 (3,36 - 8,80) | 4,91 (2,65 - 7,36) | 0,000 |
| Liver right | 9,34 (6,58 - 13,8) ^{b,c} | 7,84 (5,44 - 12,71) ^e | 7,02 (4,51 - 11,65) | 6,46 (3,82 - 11,41) | 0,000 |
| HCC | 8,57 (4,18 - 18,52) ^{b,c} | 6,41 (3,12 - 11,95) ^e | 5,63 (2,24 - 11,71) | 5,42 (1,92 - 11,85) | 0,000 |
| Spleen | 12,04 (6,96 - 21,29) ^{a,b,c} | 9,95 (5,67 - 15,74) | 9,18 (5,31 - 17,56) | 8,52 (5,08 - 15,52) | 0,000 |
| Gastric wall | 9,6 (5,05 - 14,75) ^{b,c} | 8,02 (4,02 - 12,64) | 7,08 (2,9 - 13,24) | 6,31 (3,1 - 14,14) | 0,000 |
| Pancreas | 11,93 (5,43 - 19,41) ^{a,b,c} | 8,81 (4 - 13,99) | 9,07 (4 - 21,93) | 7,36 (3,37 - 13,77) | 0,000 |
| Portal vein | 9,01 (5,96 - 11,18) ^{b,c,d} | 7,50 (4,46 - 15,06) ^e | 6,13 (2,94 - 10,08) | 5,59 (2,69 - 12,28) | 0,000 |

^aSignificantly different between FBP and ADM 3.

^bSignificantly different between FBP and ADM 4.

^cSignificantly different between FBP and ADM 5.

^dSignificantly different between ADM 3 and ADM 4.

^eSignificantly different between ADM 3 and ADM 5.

^fSignificantly different between ADM 4 and ADM 5.

Table 2

Mean signal-to-noise ratio (SNR), including ranges, for seven tissues (left liver lobe, right liver lobe, HCC, spleen, gastric wall, pancreas and portal vein) for four reconstruction algorithms (FBP, ADM 3, ADM 4, ADM 5).

| | Mean (95% confidence interval) | | | | P-value |
|--------------|---------------------------------------|-----------------------------------|----------------------|----------------------|---------|
| | FBP | ADM 3 | ADM 4 | ADM 5 | |
| SNR | | | | | |
| Liver left | 8,99 (3,21 - 14,17) ^{b,c} | 12 (4,12 - 22,93) ^e | 13,99 (5,59 - 22,93) | 15,08 (6,2 - 25,73) | 0,000 |
| Liver right | 7,81 (3,01 - 10,93) ^{b,c} | 9,33 (5,33 - 12,84) ^e | 10,54 (4,33 - 13,83) | 11,74 (6,02 - 19,76) | 0,000 |
| HCC | 11,57 (5,64 - 24,25) ^{b,c} | 15,32 (8,82 - 31,8) | 18,54 (8,07 - 36,06) | 19,3 (6,53 - 38,65) | 0,000 |
| Spleen | 8,57 (5,68 - 14,35) ^{a,b,c} | 10,6 (6,71 - 16,68) | 11,19 (7,47 - 17,32) | 12,08 (7,25 - 22,14) | 0,000 |
| Gastric wall | 7,2 (2,3 - 14,25) ^{b,c} | 8,94 (2,22 - 17,61) | 10,34 (2,39 - 19,98) | 11,25 (2,92 - 27,63) | 0,001 |
| Pancreas | 7,93 (2,71 - 23,5) ^{a,b,c} | 10,58 (4,51 - 32,06) | 10,71 (3,38 - 32,06) | 12,34 (5,48 - 29,26) | 0,000 |
| Portal vein | 11,61 (6,09 - 17,37) ^{b,c,d} | 14,55 (7,04 - 25,95) ^e | 17,85 (5,88 - 36,38) | 19,9 (7,54 - 37,31) | 0,000 |

^aSignificantly different between FBP and ADM 3.

^bSignificantly different between FBP and ADM 4.

^cSignificantly different between FBP and ADM 5.

^dSignificantly different between ADM 3 and ADM 4.

^eSignificantly different between ADM 3 and ADM 5.

^fSignificantly different between ADM 4 and ADM 5.

invasive analysis of angiogenesis [18,21] and CTP has shown benefits in the assessment and characterization of tumors [20–25]. In our study, quantitative information was helpful in differentiating between HCC tissue and nodules, as well as differentiating remaining tumor tissue from blood-flow changes after TACE. Recently, Hamdy et al. showed the potential of CTP for predicting the response to treatment for pancreatic ductal adenocarcinoma [25].

A phantom study from Gawlitza et al. [26] showed that CTP studies carried out at 70 kVp or 80 kVp are favorable in terms of radiation dose compared with studies undertaken at 130 kVp, and that the additional information might be important in patients undergoing novel targeted therapies. To obtain such information, quantitative measurements of low-dose examinations should not be different from those of a normal-dose scan. This requirement has been shown in several studies [4–9,11,13,14,27,28], including our study. Mirsadraee and colleagues [11] showed that iterative reconstruction algorithms can be used to preserve the image quality in low-dose CTP examinations, but that they can also lead to overestimation of perfusion values, especially in larger patients. This is an important fact to be aware of, and is probably due to the higher noise levels in such images. A tendency of higher image noise was seen for larger patients in our study as well.

For visual assessment to be possible, it must not be impaired by the iterative reconstruction algorithm or by use of temporal averaging methods. This phenomenon was shown in a study by Feger and colleagues [6] in which use of TAVG and iterative reconstruction degraded

objective parameters of contour sharpness in dynamic myocardial CTP. That study was carried out on a CT system from another vendor, and correction for heart motion was not addressed specifically. Present-day algorithms for motion correction might overcome this problem. This issue merits further investigation if CTP is to be considered a first-line examination.

Fischer et al. [19] showed that time-resolved CT images demonstrated superior image quality as well as better depiction of liver lesions and blood vessels. The prevalence of detection of arterialized liver lesions was also higher compared with that using raw data. Motion correction and noise reduction had been applied but multiple-band filtered images were used, and the advantages of iterative reconstructions were not examined. Our study suggests that time-averaged images reconstructed with an iterative reconstruction algorithm can be used for quantitative measurements, and that the quality of these images is superior to those using FBP.

Wang and colleagues [4] showed that there were no differences in whole-brain examinations between a low dose (80 kVp) protocol using iterative reconstruction and a low dose of contrast compared with a 100-kVp protocol with FBP reconstructions and a normal dose of contrast with regard to HU values, SNR, contrast:noise ratio, CTP values, as well as subjective and objective image quality. Those data are partly in accordance with our results with regard to objective image quality and higher HU values of the contrast agent in low-kVp examinations. The dose of contrast in our study could probably have been reduced further

because the attenuation values for contrast in our 70-kVp protocol were high. This scenario could be highly beneficial for patients with a low GFR.

Our study had three main limitations. First, we investigated only one energy level (70 kVp), so we could not compare results between different energy levels. Second, our results cannot be applied to the CT systems or post-processing software of other vendors because the reconstruction parameters and image analyses are different. This has been shown in earlier studies [29]. However, it has been shown in several studies [4–9,11,13,14,27,28] that the quantitative measurements of low-dose examinations are not different from those of a normal-dose scan. Third, image quality was evaluated only by objective measurement and not by subjective assessment by radiologists. This issue will be investigated in a future study.

5. Conclusions

The iterative image-reconstruction algorithm used in our study did not affect the quantitative measurements or time-attenuation curves of tissues in the upper abdomen. Image noise was lower, but the SNR was higher, for iterative reconstructions with higher strength of noise reduction.

Funding

This work was supported by the County council of Östergötland, Sweden (ALF) and Medical Research Council of Southeast Sweden (FORSS).

CRediT authorship contribution statement

Mischa Woisetschläger: Conceptualization, Methodology, Formal analysis, Investigation, Writing - original draft, Writing - review & editing, Visualization, Supervision, Project administration. **Lilian Henriksson:** Conceptualization, Methodology, Formal analysis, Investigation, Writing - review & editing. **Wolf Bartholomae:** Conceptualization, Methodology, Formal analysis, Investigation, Writing - review & editing. **Thomas Gasslander:** Conceptualization, Methodology, Formal analysis, Investigation, Writing - review & editing. **Bergthor Björnsson:** Conceptualization, Methodology, Formal analysis, Investigation, Writing - review & editing. **Per Sandström:** Conceptualization, Methodology, Formal analysis, Investigation, Writing - review & editing.

Declaration of Competing Interest

The authors have no conflict of interest in this work

Acknowledgements

We thank Petter Quick for his valuable help in discussing the protocol and performing the examinations. We also thank Ulrike Haberland for her valuable help in defining the protocol.

References

- [1] V. Dushyant Sahani, Perfusion CT: an overview of technique and clinical applications, *Intl. Soc. Mag. Reson. Med.* 18 (2010).
- [2] M.K. Kalra, M. Woisetschläger, N. Dahlström, S. Singh, S. Digumarthy, S. Do, H. Pien, P. Quick, B. Schmidt, M. Sedlmair, J.-A.O. Shepard, A. Persson, Sinogram-affirmed iterative reconstruction of low-dose chest CT: effect on image quality and radiation dose, *AJR Am. J. Roentgenol.* 201 (2013) W235–244, <https://doi.org/10.2214/AJR.12.9569>.
- [3] M.K. Kalra, M. Woisetschläger, N. Dahlström, S. Singh, M. Lindblom, G. Choy, P. Quick, B. Schmidt, M. Sedlmair, M.A. Blake, A. Persson, Radiation dose reduction with sinogram affirmed iterative reconstruction technique for abdominal computed tomography, *J. Comput. Assist. Tomogr.* 36 (2012) 339–346, <https://doi.org/10.1097/RCT.0b013e31825586c0>.
- [4] T. Wang, Y. Gong, Y. Shi, R. Hua, Q. Zhang, Feasibility of dual-low scheme combined with iterative reconstruction technique in acute cerebral infarction volume CT whole brain perfusion imaging, *Exp. Ther. Med.* 14 (2017) 163–168, <https://doi.org/10.3892/etm.2017.4451>.
- [5] J.M. Niesten, I.C. Van Der Schaaf, A.J. Riordan, H.W.A.M. De Jong, A.D. Horsch, D. Eijspaart, E.J. Smit, W.P.T.M. Mali, B.K. Velthuis, Radiation dose reduction in cerebral CT perfusion imaging using iterative reconstruction, *Eur. Radiol.* 24 (2014) 484–493, <https://doi.org/10.1007/s00330-013-3042-4>.
- [6] S. Feger, C. Kendziorra, S. Lukas, A. Shaban, B. Bokelmann, E. Zimmermann, M. Rief, M. Dewey, Effect of iterative reconstruction and temporal averaging on contour sharpness in dynamic myocardial CT perfusion: sub-analysis of the prospective 4D CT perfusion pilot study, *PLoS One* 13 (2018) 1–17, <https://doi.org/10.1371/journal.pone.0205922>.
- [7] N.M. Bhave, V. Mor-Avi, N. Kachenoura, B.H. Freed, M. Vannier, K. Dill, R.M. Lang, A.R. Patel, Analysis of myocardial perfusion from vasodilator stress computed tomography: does improvement in image quality by iterative reconstruction lead to improved diagnostic accuracy? *J. Cardiovasc. Comput. Tomogr.* 8 (2014) 238–245, <https://doi.org/10.1016/j.jcct.2014.04.008>.
- [8] B.M. Gramer, D. Muenzel, V. Leber, A.K. Von Thaden, H. Feussner, A. Schneider, M. Vembar, N. Soni, E.J. Rummeny, A.M. Huber, Impact of iterative reconstruction on CNR and SNR in dynamic myocardial perfusion imaging in an animal model, *Eur. Radiol.* 22 (2012) 2654–2661, <https://doi.org/10.1007/s00330-012-2525-z>.
- [9] Y. Tanabe, T. Kido, A. Kurata, T. Kouchi, T. Hosokawa, H. Nishiyama, N. Kawaguchi, T. Kido, T. Uetani, T. Mochizuki, Impact of knowledge-based iterative model reconstruction on image quality and hemodynamic parameters in dynamic myocardial computed tomography perfusion using low-tube-voltage scan: a feasibility study, *J. Comput. Assist. Tomogr.* 43 (2019) 811–816, <https://doi.org/10.1097/RCT.0000000000000914>.
- [10] Y. Ohno, H. Koyama, Y. Fujisawa, T. Yoshikawa, H. Inokawa, N. Sugihara, S. Seki, K. Sugimura, Hybrid Type iterative reconstruction method vs. Filter back projection method: capability for radiation dose reduction and perfusion assessment on dynamic first-pass contrast-enhanced perfusion chest area-detector CT, *Eur. J. Radiol.* 85 (2016) 164–175, <https://doi.org/10.1016/j.ejrad.2015.11.010>.
- [11] S. Mirsadraee, N.W. Weir, S. Connolly, J.T. Murchison, J.H. Reid, N. Hirani, M. Connell, E.J. Van Beek, Feasibility of radiation dose reduction using AIDR-3D in dynamic pulmonary CT perfusion, *Clin. Radiol.* 70 (2015) 844–851, <https://doi.org/10.1016/j.crad.2015.04.004>.
- [12] N. Negi, T. Yoshikawa, Y. Ohno, Y. Somya, T. Sekitani, N. Sugihara, H. Koyama, T. Kanda, N. Kanata, T. Murakami, H. Kawamitsu, K. Sugimura, Hepatic CT perfusion measurements: a feasibility study for radiation dose reduction using new image reconstruction method, *Eur. J. Radiol.* 81 (2012) 3048–3054, <https://doi.org/10.1016/j.ejrad.2012.04.024>.
- [13] Q. Xie, J. Wu, Y. Tang, Y. Dou, S. Hao, F. Xu, X. Feng, Z. Liang, Whole-organ CT perfusion of the pancreas: impact of iterative reconstruction on image quality, perfusion parameters and radiation dose in 256-slice CT-preliminary findings, *PLoS One* 8 (2013) 4–11, <https://doi.org/10.1371/journal.pone.0080468>.
- [14] D. Prezzi, V. Goh, S. Virdi, S. Mallett, C. Grierson, D.J. Breen, Adaptive statistical iterative reconstruction improves image quality without affecting perfusion CT quantitation in primary colorectal cancer, *Eur. J. Radiol. Open* 4 (2017) 69–74, <https://doi.org/10.1016/j.ejro.2017.05.003>.
- [15] K.T. Bae, Intravenous contrast medium administration and scan timing at CT: considerations and approaches, *Radiology* 256 (2010) 32–61, <https://doi.org/10.1148/radiol.10090908>.
- [16] M. Rengo, D. Bellini, C.N. De Cecco, M. Osmani, F. Vecchietti, D. Caruso, M.M. Maceroni, P. Lucchesi, F. Iafrate, P. Paolantonio, R. Ferrari, A. Laghi, The optimal contrast media policy in CT of the liver. Part I: Technical notes, *Acta Radiol.* 52 (2011) 467–472, <https://doi.org/10.1258/ar.2011.100499>.
- [17] M. Rengo, D. Bellini, C.N. De Cecco, M. Osmani, F. Vecchietti, D. Caruso, M.M. Maceroni, P. Lucchesi, F. Iafrate, E. Palombo, P. Paolantonio, R. Ferrari, A. Laghi, The optimal contrast media policy in CT of the liver. Part II: clinical protocols, *Acta Radiol.* 52 (2011) 473–480, <https://doi.org/10.1258/ar.2011.100500>.
- [18] E. Klotz, U. Haberland, G. Glatting, S.O. Schoenberg, C. Fink, U. Attenberger, T. Henzler, Technical prerequisites and imaging protocols for CT perfusion imaging in oncology, *Eur. J. Radiol.* (2015) 1–9, <https://doi.org/10.1016/j.ejrad.2015.06.010>.
- [19] M. a Fischer, B. Leidner, N. Kartalis, A. Svensson, P. Aspelin, N. Albiin, T.B. Brismar, Time-resolved computed tomography of the liver: retrospective, multi-phase image reconstruction derived from volumetric perfusion imaging, *Eur. Radiol.* 24 (2014) 151–161, <https://doi.org/10.1007/s00330-013-2992-x>.
- [20] K.a. Miles, T.-Y. Lee, V. Goh, E. Klotz, C. Cuenod, S. Bidas, A.M. Groves, M.P. Hayball, R. Alonzi, T. Brunner, Current status and guidelines for the assessment of tumour vascular support with dynamic contrast-enhanced computed tomography, *Eur. Radiol.* 22 (2012) 1430–1441, <https://doi.org/10.1007/s00330-012-2379-4>.
- [21] G. Petralia, L. Bonello, S. Viotti, L. Preda, G. Andrea, M. Bellomi, REVIEW CT Perfusion in Oncology: How to Do It, (2010), pp. 8–19, <https://doi.org/10.1102/1470-7330.2010.0001>.
- [22] M. Hatem, K.A. Shalaby, Ali Shehata, CT perfusion in hepatocellular carcinoma: is it reliable? *Egypt. J. Radiol. Nucl. Med.* 48 (2017) 791–798, <https://doi.org/10.1016/j.ejnm.2017.07.013>.
- [23] H. Ogul, M. Kantarci, B. Genc, B. Pirimoglu, N. Cullu, Y. Kizrak, O. Yilmaz, N. Karabulut, Perfusion CT imaging of the liver: review of clinical applications, *Diagn. Interv. Radiol.* 20 (2014) 379–389, <https://doi.org/10.5152/dir.2014.13396>.
- [24] S.H. Kim, A. Kamaya, J.K. Willmann, CT perfusion of the liver: principles and

- applications in oncology, *Radiology* 272 (2014) 322–344, <https://doi.org/10.1148/radiol.14130091>.
- [25] A. Hamdy, Y. Ichikawa, Y. Toyomasu, M. Nagata, N. Nagasawa, Y. Nomoto, H. Sami, H. Sakuma, Perfusion CT to assess response to neoadjuvant chemotherapy and radiation therapy in pancreatic ductal adenocarcinoma: initial experience, *Radiology* 292 (2019) 628–635, <https://doi.org/10.1148/radiol.2019182561>.
- [26] J. Gawlitza, H. Haubenreisser, M. Meyer, C. Hagelstein, S. Sudarski, S.O. Schoenberg, T. Henzler, Comparison of organ-specific-radiation dose levels between 70 kVp perfusion CT and standard tri-phasic liver CT in patients with hepatocellular carcinoma using a Monte-Carlo-Simulation-based analysis platform, *Eur. J. Radiol. Open* 3 (2016) 95–99, <https://doi.org/10.1016/j.ejro.2016.04.003>.
- [27] N. Negi, T. Yoshikawa, Y. Ohno, Y. Somiya, T. Sekitani, N. Sugihara, H. Koyama, T. Kanda, N. Kanata, T. Murakami, H. Kawamitsu, K. Sugimura, Hepatic CT perfusion measurements: a feasibility study for radiation dose reduction using new image reconstruction method, *Eur. J. Radiol.* 81 (2012) 3048–3054, <https://doi.org/10.1016/j.ejrad.2012.04.024>.
- [28] P.J. Navin, B. Kim, M.L. Wells, A. Khandelwal, A.F. Halaweish, T.R. Moen, M.P. Johnson, S. Mccollough, Y. Suk, L. Shuai, L. Cynthia, J.G. Fletcher, Reducing radiation dose for multi - phase contrast - enhanced dual energy renal CT : pilot study evaluating prior iterative reconstruction, *Abdom. Radiol.* 44 (2019) 3350–3358, <https://doi.org/10.1007/s00261-019-02150-9>.
- [29] E.A.S. Bretas, U.S. Torres, L.R. Torres, D. Bekhor, C.F.S. Filho, D.J. Racy, L. Faggioni, G. D'ippolito, Is liver perfusion CT reproducible? A study on intraand interobserver agreement of normal hepatic haemodynamic parameters obtained with two different software packages, *Br. J. Radiol.* 90 (2017), <https://doi.org/10.1259/bjr.20170214>.